

# Spatial Profile of the Emission from Pulsar Wind Nebulae with steady-state 1D Modeling



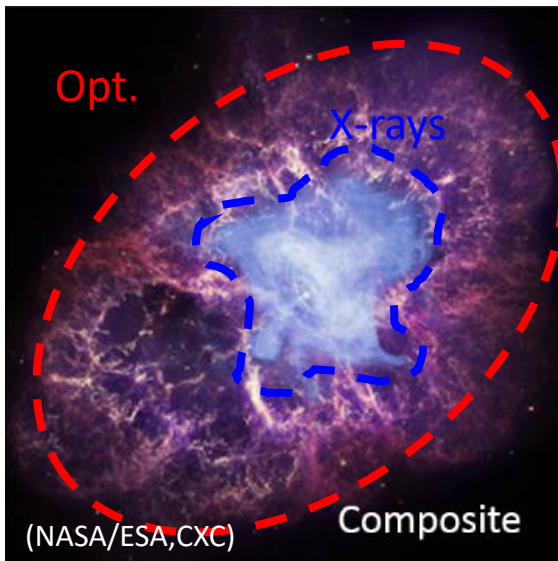
**Wataru Ishizaki**

( Department of Physics, Graduate School of Science,  
The University of Tokyo )

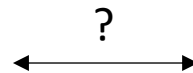
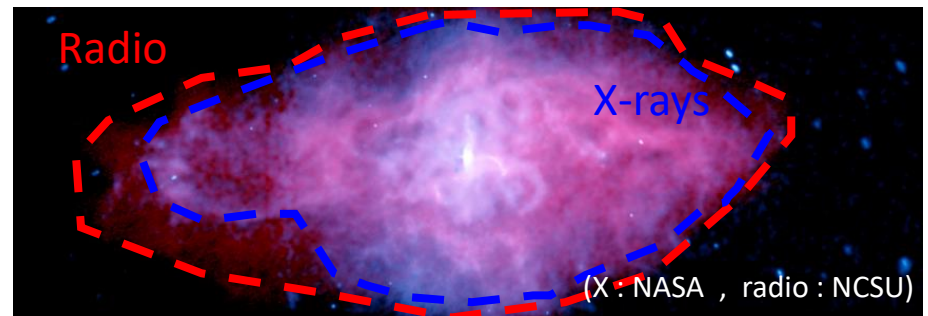
# Abstract

- The pulsar releases its rotational energy as highly relativistic wind
- This produces a pc-scale nebula, called as Pulsar Wind Nebula (PWN)
- The “standard model” of PWN based on Crab found general acceptance
- BUT the PWN which exhibits different feature from Crab is found
- We calculate both the entire spectrum and the spatial structure of emission spontaneously and examine the “standard model”

Crab Nebula



3C 58



The size of Crab nebula shrink with increasing frequency.  
This fact is interpreted by synchrotron cooling.  
BUT 3C 58 does not appear this feature...

# Introduction

# Introduction –Pulsar Wind Nebulae–

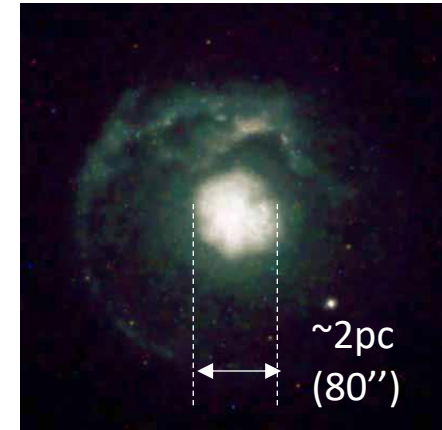
- Extended objects around the isolated pulsar
  - Center-filled morphology
  - Physical scale  $\sim$  a few pc
- Very broad non-thermal spectrum from radio to TeV- $\gamma$  rays
  - Synchrotron and Inverse Compton radiation from shocked pulsar wind
- e.g. Crab Nebula (as known as “M1”)

3C 58 (Blue :X , Red : Radio)

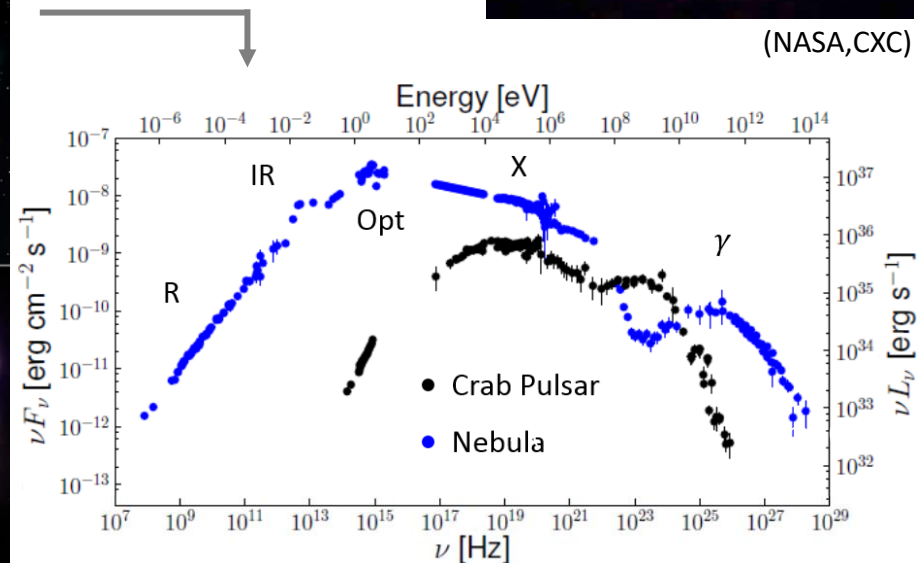
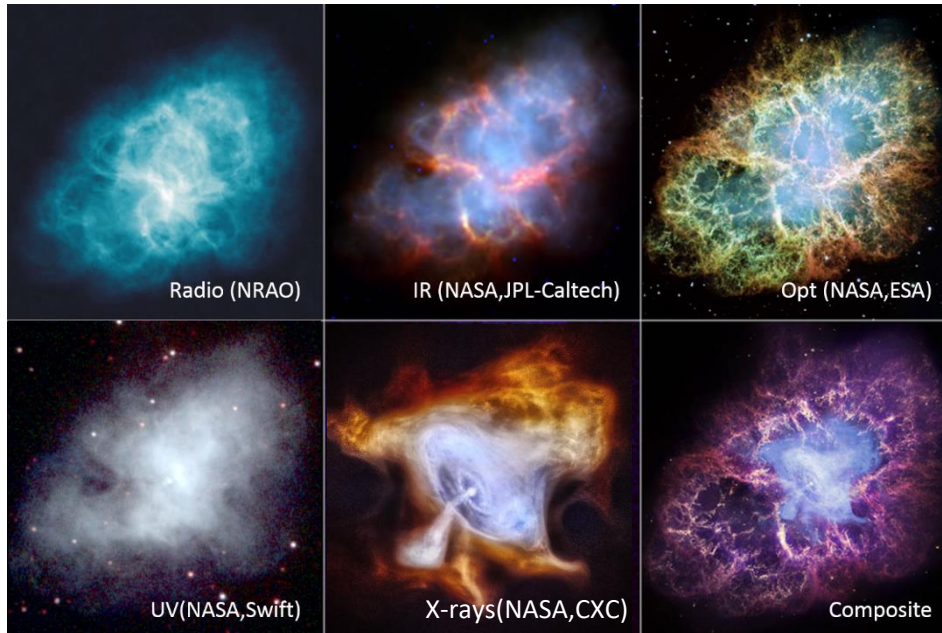


(X : NASA , radio : NCSU)

G21.5-0.9



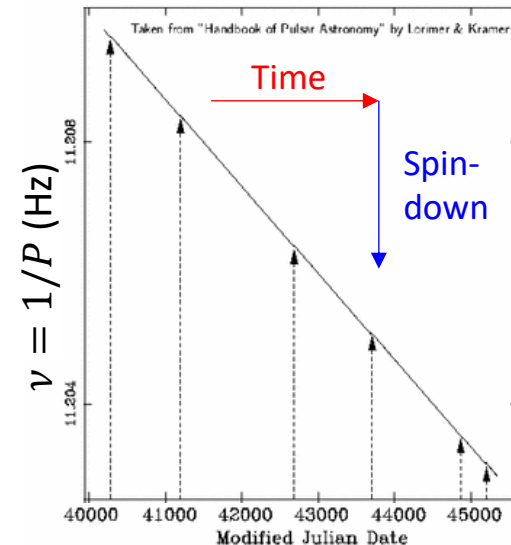
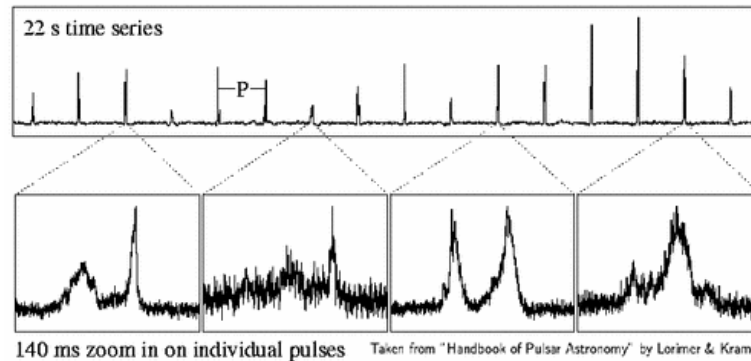
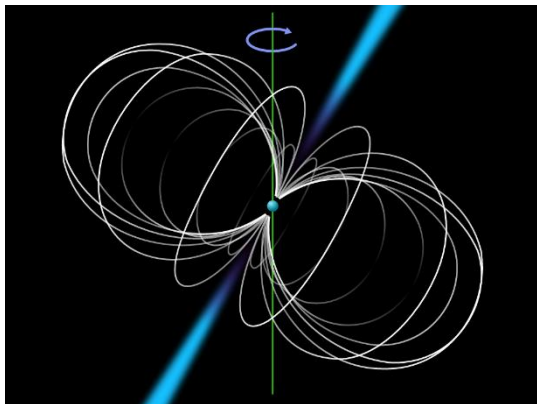
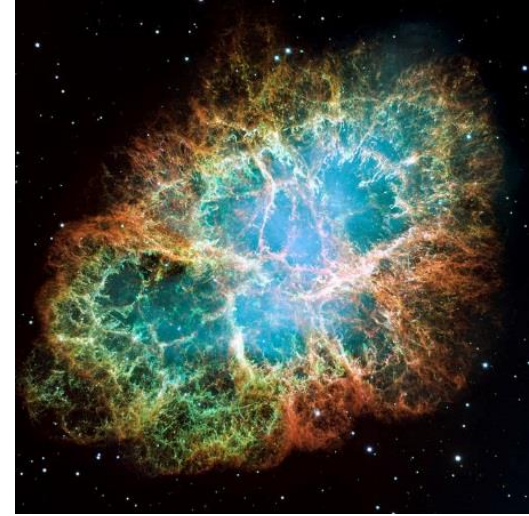
(NASA,CXC)



(Buhler & Blandford , 2014)

# Introduction –Pulsar Wind Nebulae-

- Rotation-Powered Pulsar
  - Periodic radiation :  $P \sim 1s$
  - Magnetic braking by strong  $B \sim 10^{12}G$
- Pulsar releases its rotational energy
  - Time derivative of P is well observed :  $\dot{P} \sim 10^{-(12-13)} s s^{-1}$
  - $L_{sd} = |I\Omega\dot{\Omega}| = 5 \times 10^{38} \text{erg/s} \left(\frac{P}{33ms}\right)^{-3} \left(\frac{\dot{P}}{4.21 \times 10^{-13}}\right)$  (Crab pulsar)
- Pulsar Wind Nebula(PWN) is driven by pulsar
  - Pulse luminosity  $\sim 1\% \times L_{sd} \ll L_{sd}$
  - (Nebula luminosity)+(Expanding power)  $\sim L_{sd}$
  - Most of  $L_{sd}$  is injected to PWN





# Introduction –Pulsar Wind Nebulae-

Blue : X-rays

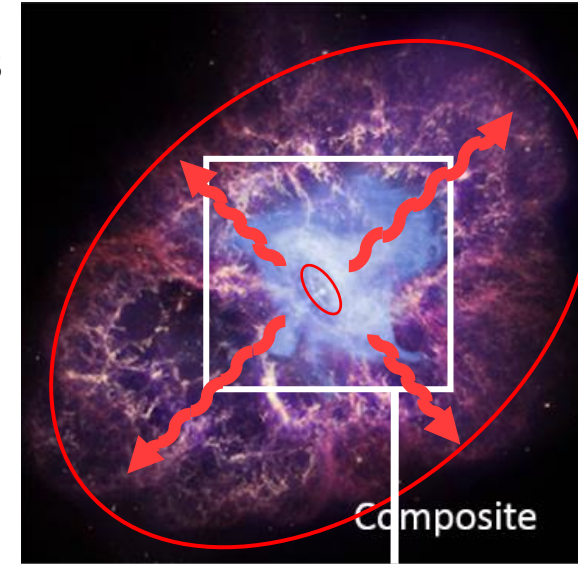
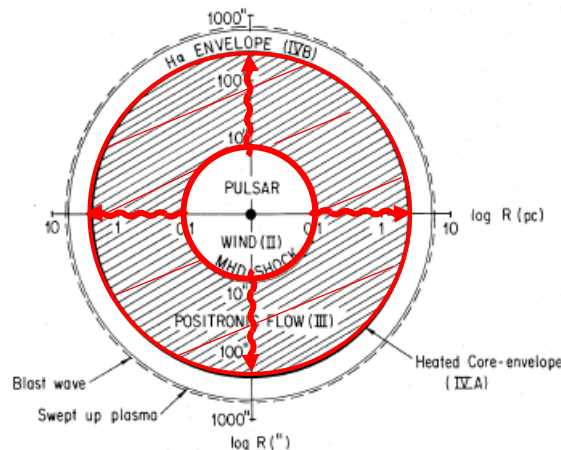
Red : Opt.

- Pulsar Wind

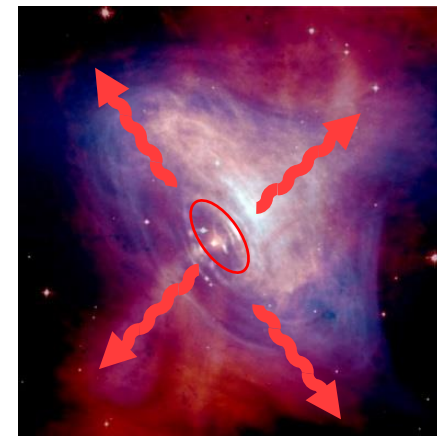
- Outflow which brings out pulsar rotational energy
- Highly relativistic wind (bulk  $\Gamma \sim 10^6$ ) consists of  $e^\pm$
- The strong shock is formed due to the interaction with interstellar matter

- Kennel & Coroniti (1984); Standard model for PWN (hereafter KC model)

- 1D and steady state MHD model
- The non-thermal  $e^\pm$  are produced by shock acceleration
- Due to the effect of radiative cooling, the emission region becomes narrow with increasing frequency



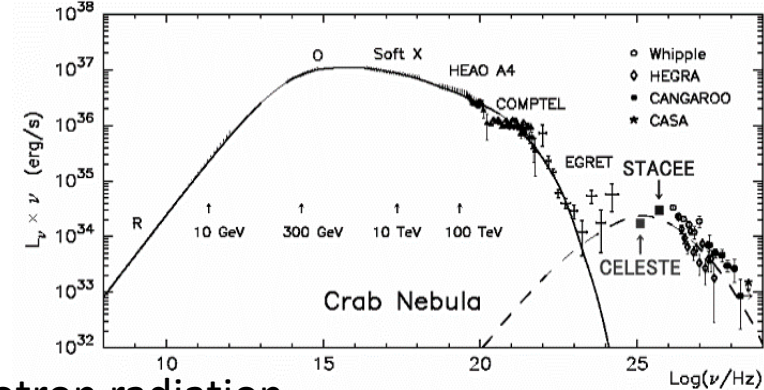
(NASA/ESA)



(NASA/CXC/SAO)

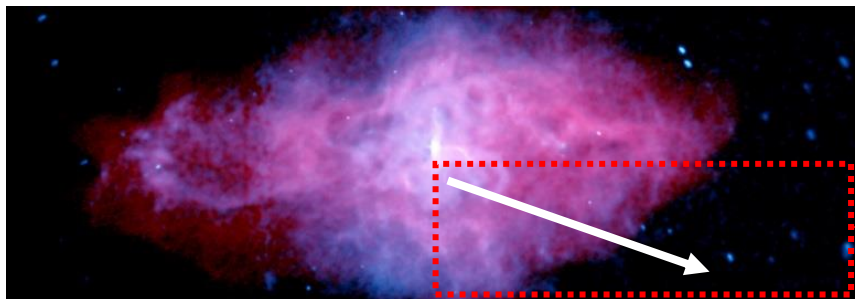
# Introduction -1D steady model-

- Previous studies of 1D steady model for PWN
  - Kennel & Coroniti (1984) ; MHD model + synchrotron radiation
  - Atoyan & Aharonian (1996)
    - Reproducing the whole spectrum of Crab nebula by considering the Inverse Compton
- Raised problems of 1D steady model
  - KC model is ONLY confirmed by Crab nebula
    - Can KC model explain a spectrum of general PWN?
  - There are some X-ray PWNe that extend the same as radio
    - Different behavior from Crab nebula...

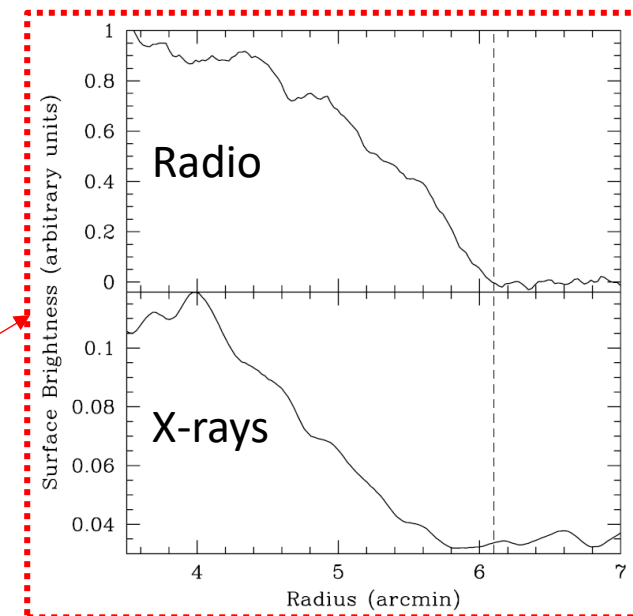


Entire spectrum  
+  
Spatial structure of emission

Can we reproduce these simultaneously?



↑3C58 (X(blue) : NASA , radio(red) : NCSU)



Model



# Model –Overview–

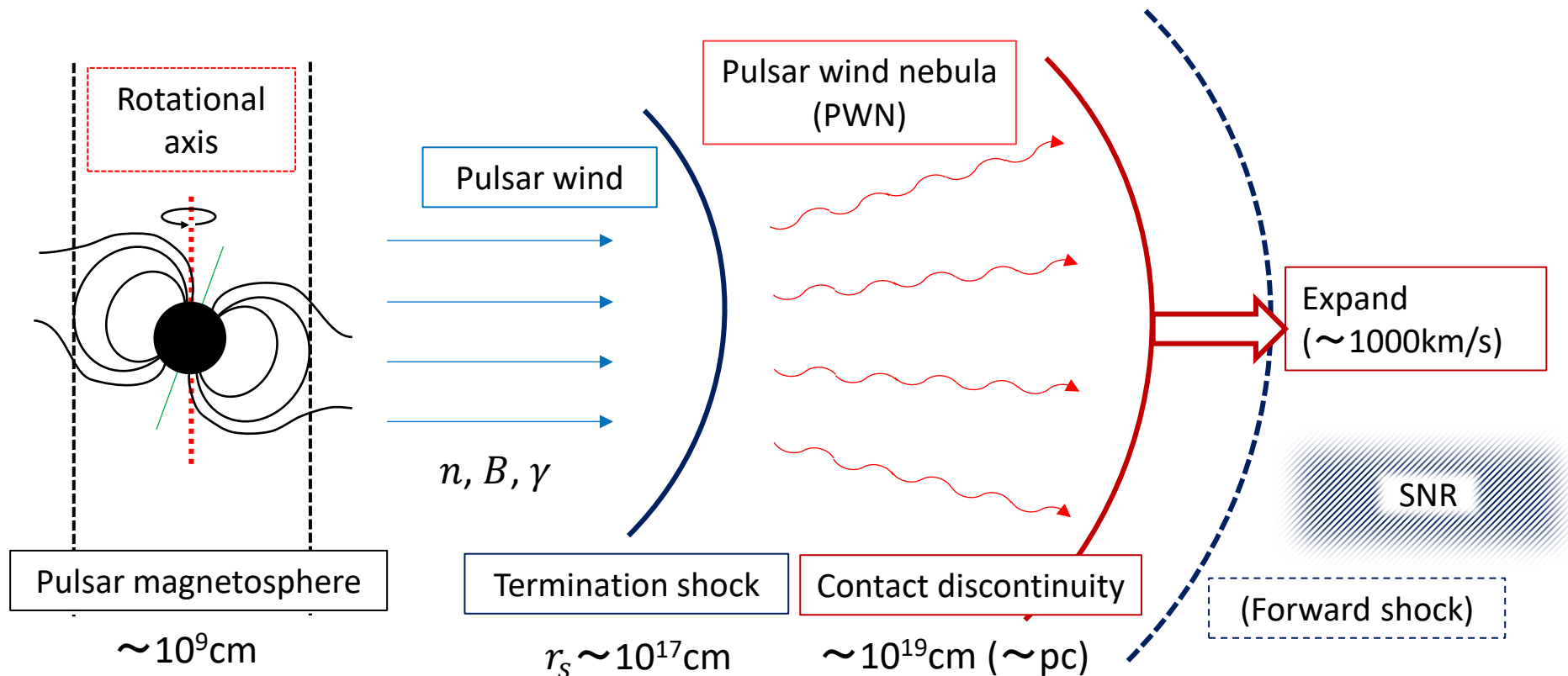
- Schematic view of KC model

- Pulsar wind forms the shock structure
- Downstream flow is free stream
- Assuming that the energy distribution at  $r_s$
- Propagating in PWN with radiative cooling

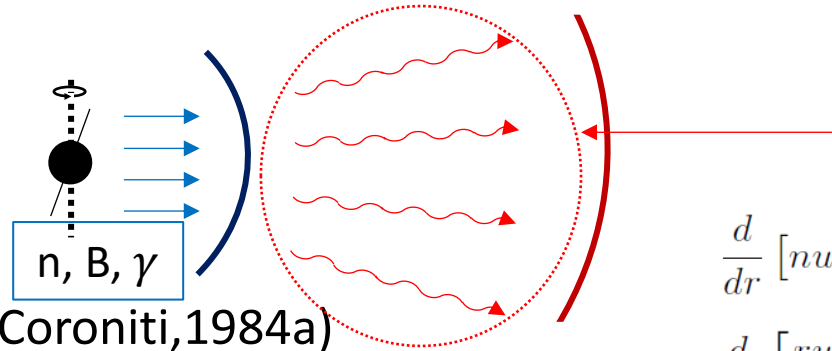
⇒ Jump condition at termination shock

⇒ Sub-sonic steady flow

⇒ Evolution of energy distribution



# Model –Flow Solution–



- MHD model of PWN (Kennel & Coroniti, 1984a)
  - Up-stream : Pulsar wind (unshocked)
    - Assumptions : Cold Plasma, toroidal field & Highly relativistic wind
  - $\sigma$  parameter
    - Assuming that the downstream is adiabatic flow, downstream is only characterized by (up-stream)  $\sigma$  parameter.

$$\sigma = \frac{B_1^2 / 4\pi}{n_1 u_1 \gamma_1 m c^2} = \frac{(\text{Poynting flux})}{(\text{particle energy flux})}$$

$$\frac{d}{dr} [n u r^2] = 0$$

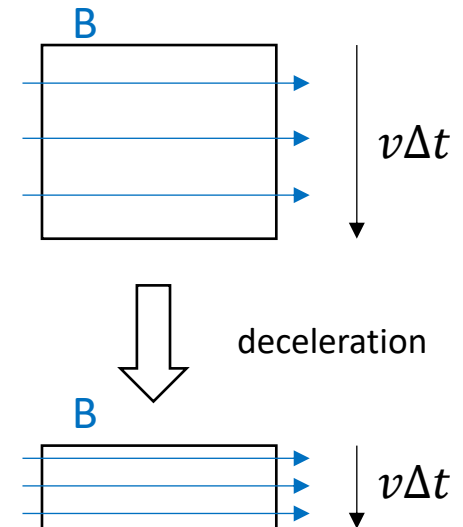
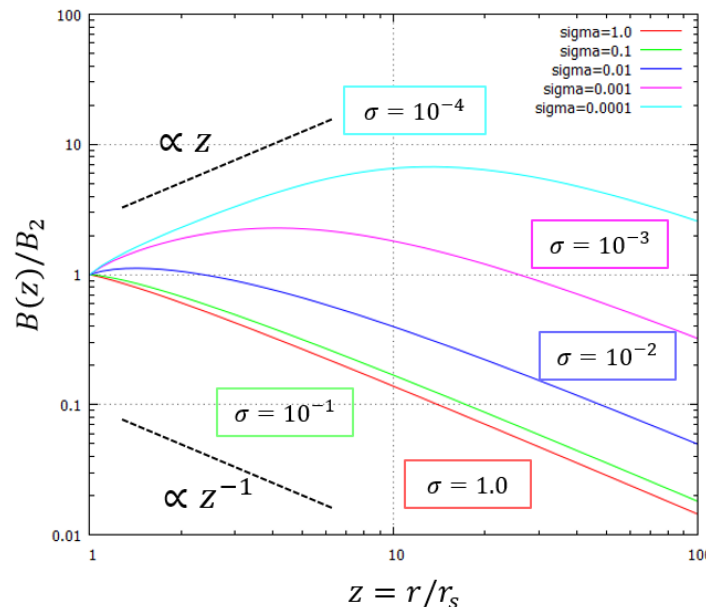
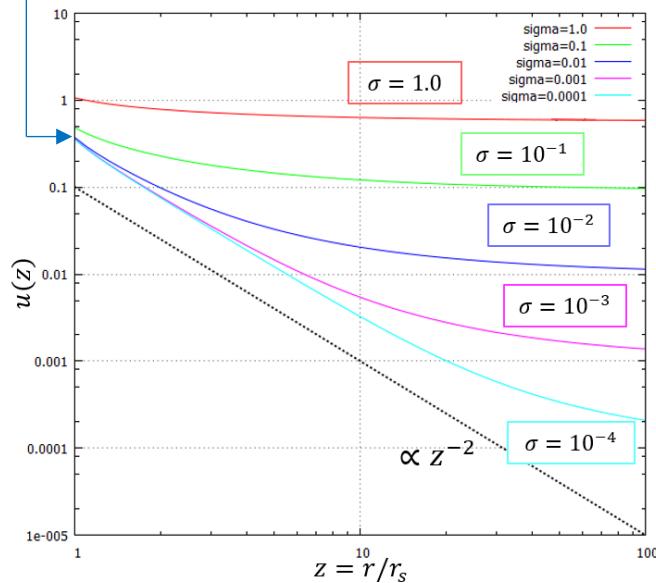
$$\frac{d}{dr} \left[ \frac{r u B}{\gamma} \right] = 0$$

$$n u r^2 \frac{d}{dr} \left[ \gamma \mu + \frac{B^2}{4\pi n \gamma} \right] = 0$$

$$\frac{d}{dr} (u r^2 n e) + p \frac{d}{dr} (u r^2) = 0$$

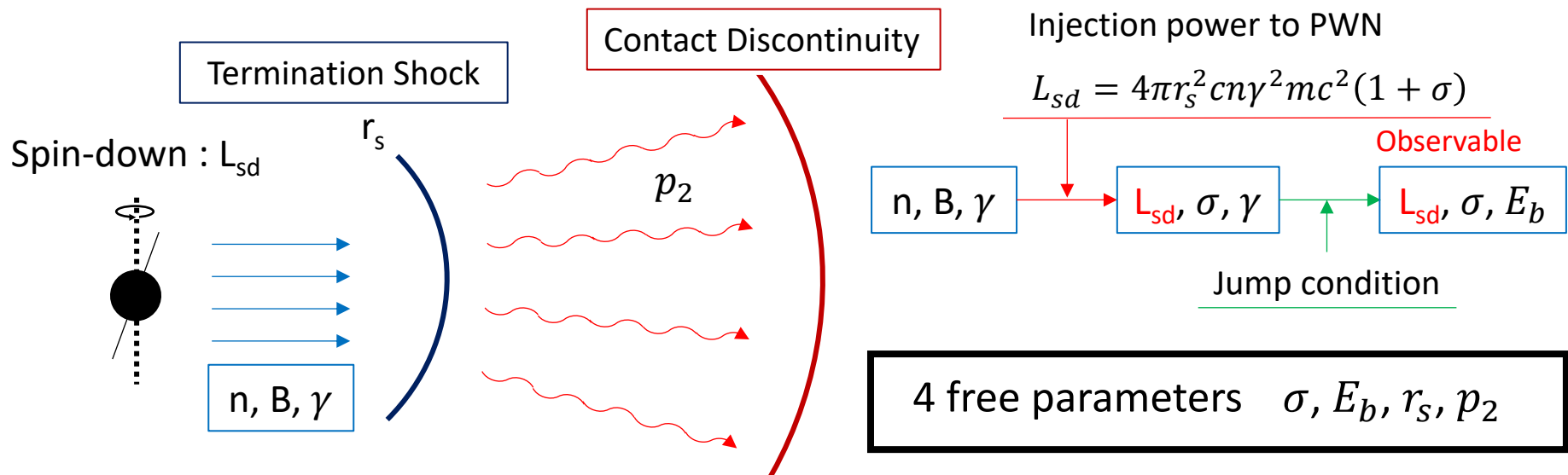
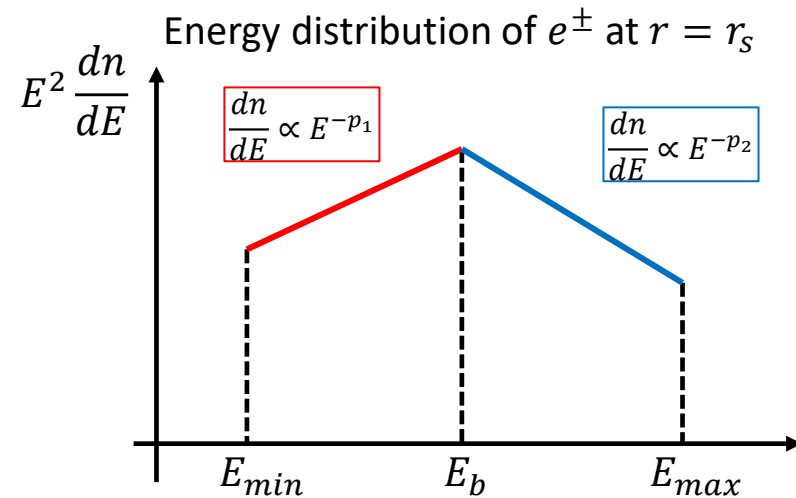
$$\mu = m c^2 + \frac{\Gamma_c}{\Gamma_c - 1} \left( \frac{P}{n} \right)$$

$$v \sim \frac{c}{3}$$



# Model –Injection & Parameters–

- Boundary condition
  - Presuming broken power-law form
- Assumption/Observable quantities
  - $E_{\min} = 10mc^2$  is fixed
  - $E_{\max}$  is determined by “size limited” :  $E_{\max} = eB_{\text{up}}r_s$
  - $p_1$  is corresponding to radio index, which is well observed. (e.g. Crab  $p_1 \sim 1.6$ )
  - All the spin-down power  $L_{sd}$  is converted to non-thermal  $e^\pm$  and flow kinetic energy



# Model –Energy distribution & Radiation–

- Evolution of non-thermal  $e^\pm$

- $n(E,r)$  : the energy spectrum of  $e^\pm$  at radius  $r$

$$\frac{\partial n}{\partial t} + u \frac{\partial n}{\partial r} = \frac{\partial}{\partial E} (Q_{\text{syn}} E^2 n) + \frac{\partial}{\partial E} (Q_{\text{IC}} E^2 n) + \frac{\partial}{\partial E} \left( \frac{c}{3r^2} \frac{d}{dr} (ur^2) E n \right) - \frac{c}{r^2} \frac{d}{dr} (ur^2) n$$

Convective derivative

Synchrotron cooling

IC cooling

Adiabatic cooling

Volume expansion

Flow solution given by MHD model

- Calculation of photon spectrum

- Synchrotron radiation

- The magnetic field  $B(r)$  given by flow solution

- Inverse Compton scattering

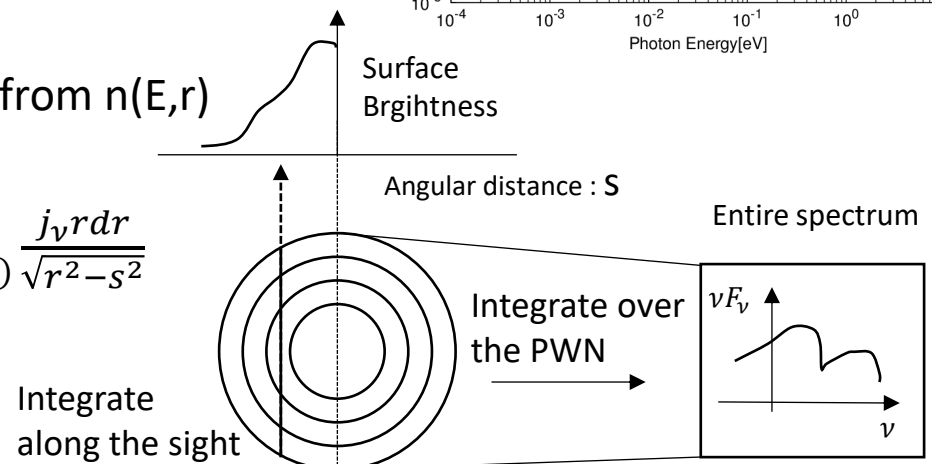
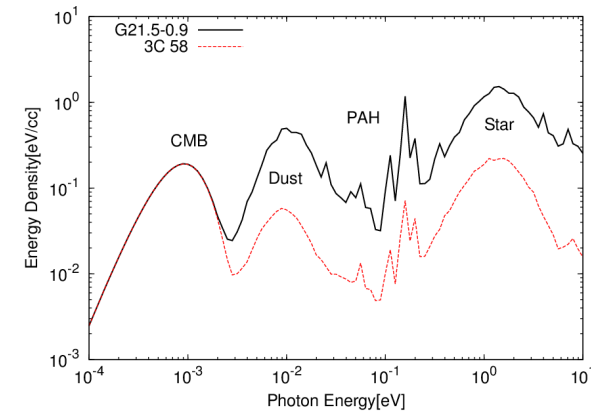
- The model of seed photon is taken from GALPROP
- Fully taking into account the Klein-Nishina effect

- Observable quantities

- The spectral emissivity  $j_\nu$  is obtained from  $n(E,r)$

- Flux :  $F_\nu = \frac{1}{4\pi D^2} \int_{r_S}^{r_N} j_\nu 4\pi r^2 dr$

- Surface brightness :  $B_\nu(s) = \int_{\min(r_S, s)}^{r_N} \frac{j_\nu r dr}{\sqrt{r^2 - s^2}}$



# Test Calculation



# Test Calculation -configurations-

$$t_{\text{adv}} \equiv \int_{r_s}^{r_N} \frac{dr}{cu(r)}$$

## Parameters

- $\sigma = 1.0 \times 10^{-4}$
- $r_s = 0.1[\text{pc}]$
- $E_b = 10^5 mc^2$
- $p_2 = 2.5$

Free Parameter

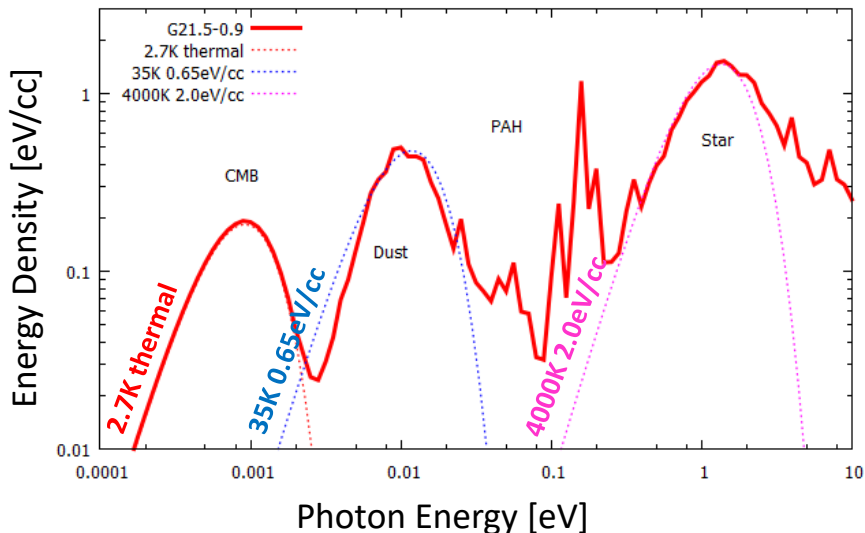
- $L_{sd} = 10^{38}[\text{erg/s}]$
- $E_{\text{min}} = 10 mc^2$
- $p_1 = 1.1$
- $D = 2[\text{kpc}]$
- $r_N = 2[\text{pc}]$

Adopted Parameter

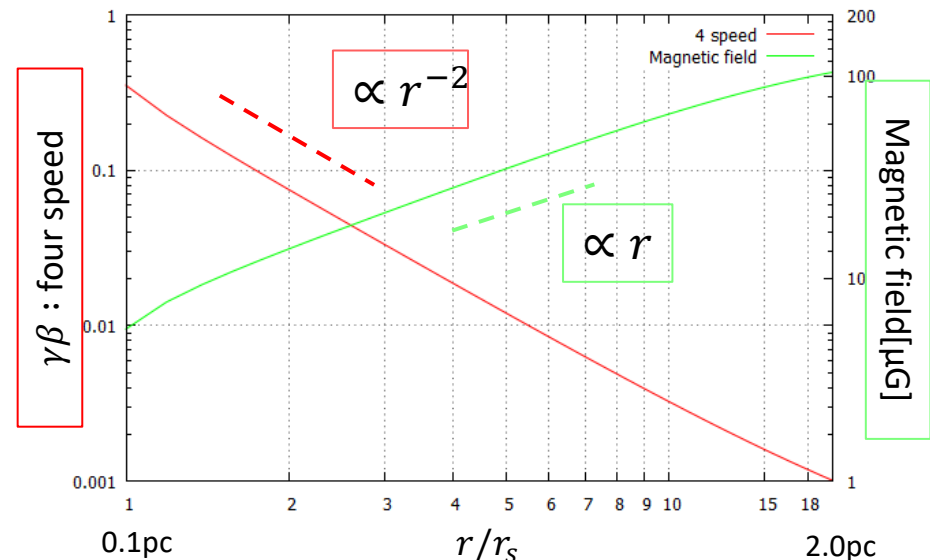
- $E_{\text{max}} = 3.4 \times 10^8 mc^2$
- $B_1 = 1.9[\mu\text{G}]$
- $n_1 = 4.5 \times 10^{-12}[\text{/cc}]$
- $t_{\text{adv}} = 2411[\text{yr}]$

Obtained parameter

## Interstellar Radiation field



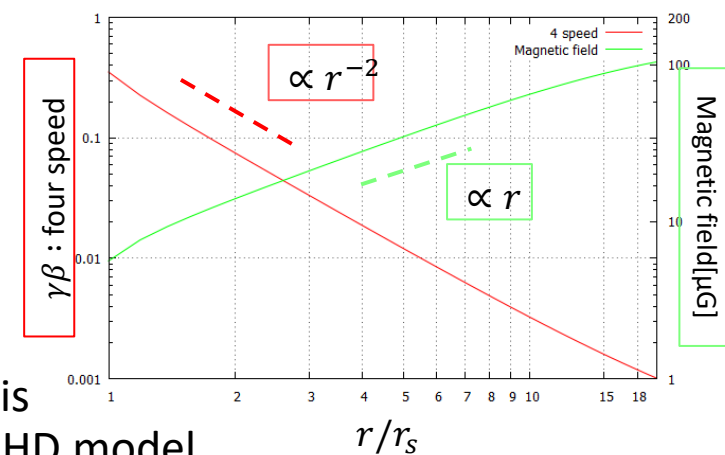
## Flow structure



# Test Calculation -energy spectrum-

- Energy spectrum of non-thermal  $e^\pm$

- At  $r = r_s$ , absolute value of distribution function is determined so as to keep the consistency with MHD model
- So the synchrotron life-time  $\propto E^{-1}$ , maximum energy of spectrum becomes lower with increasing radius  $r$
- Effect of inverse Compton cooling is negligible
- Adiabatic cooling appears as a simultaneous energy-loss



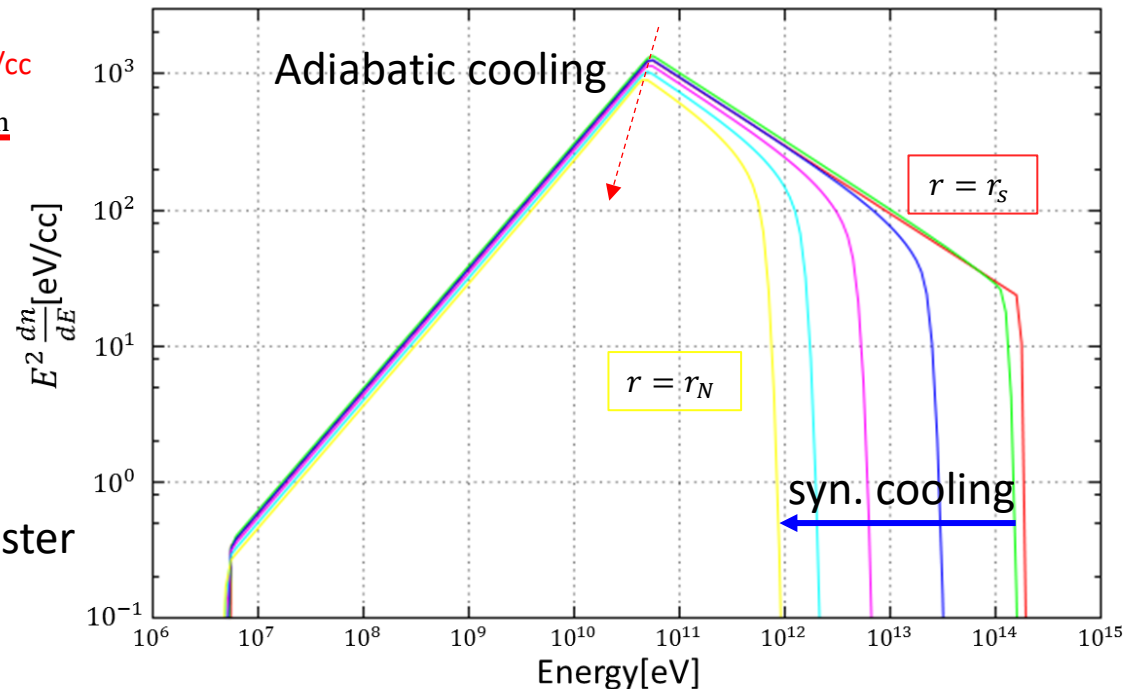
$$\left(\frac{dE}{dt}\right)_{\text{syn}} = \frac{4}{3} \sigma_T c \gamma^2 \underline{U_B}^{160\text{eV/cc}} \quad \left(\frac{dE}{dt}\right)_{\text{IC}} \sim \frac{4}{3} \sigma_T c \gamma^2 \underline{U_{\text{ph}}}^{2\text{eV/cc}}$$

$U_B \gg U_{\text{ph}}$  is established

$\Rightarrow$  Synchrotron cooling dominated

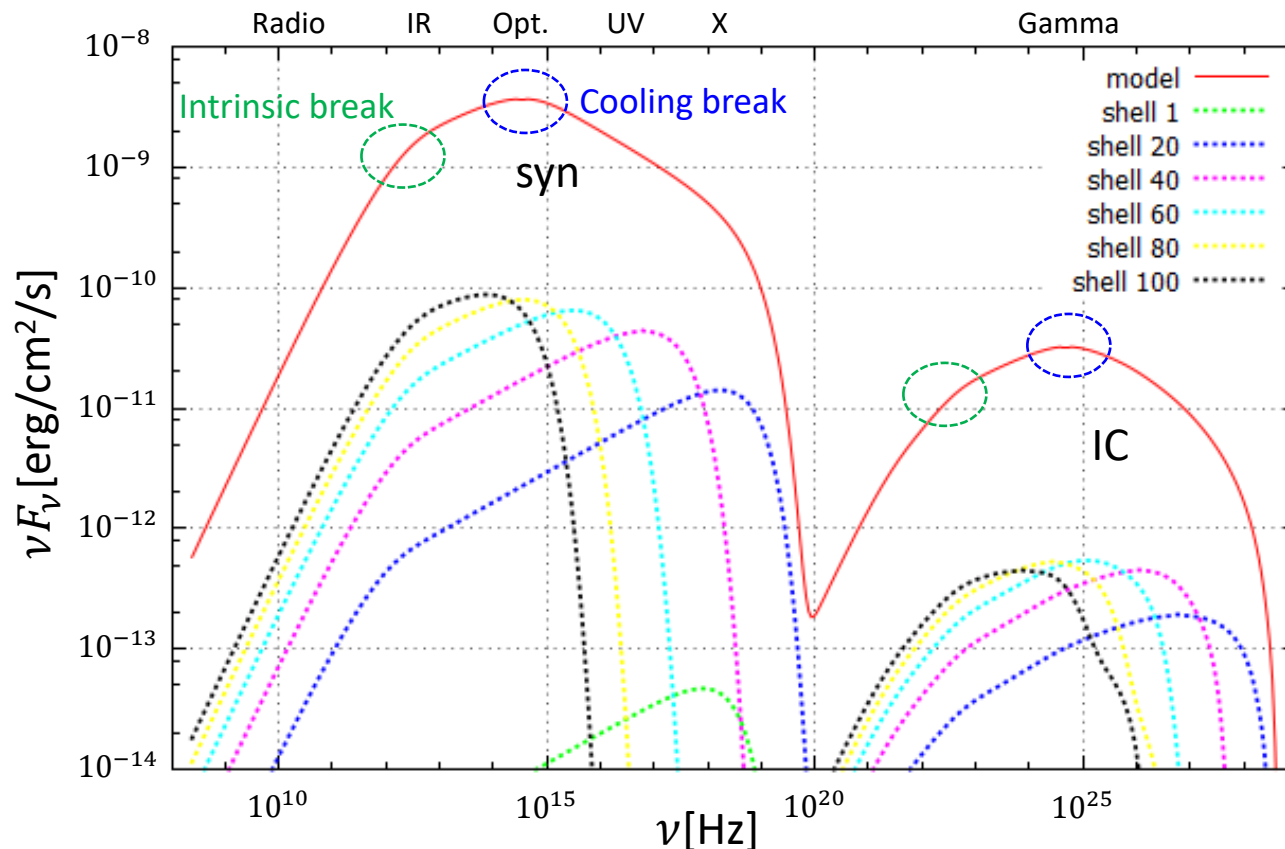
$$t_{\text{cool}} \sim \frac{E}{\left(\frac{dE}{dt}\right)_{\text{syn}}} \propto E^{-1}$$

$\Rightarrow$  Higher energy electrons exhaust faster



# Test Calculation -Spectrum-

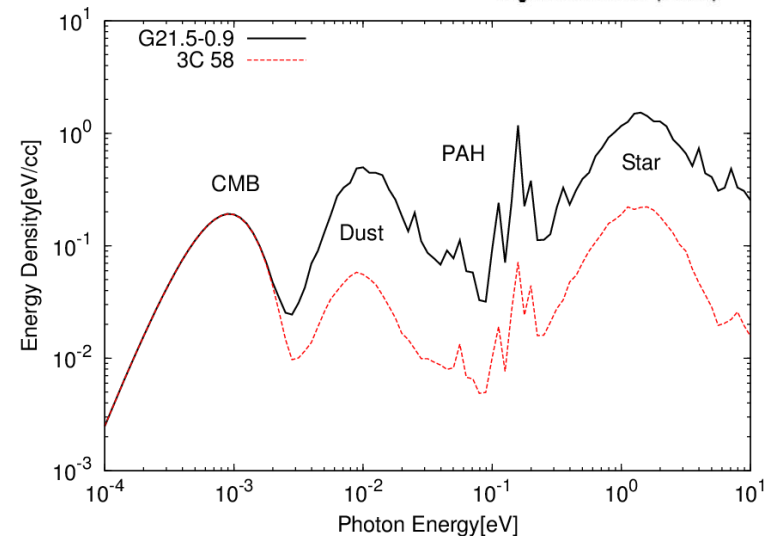
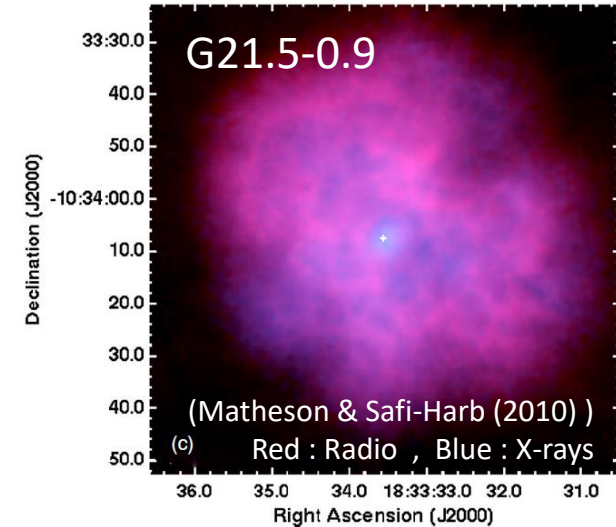
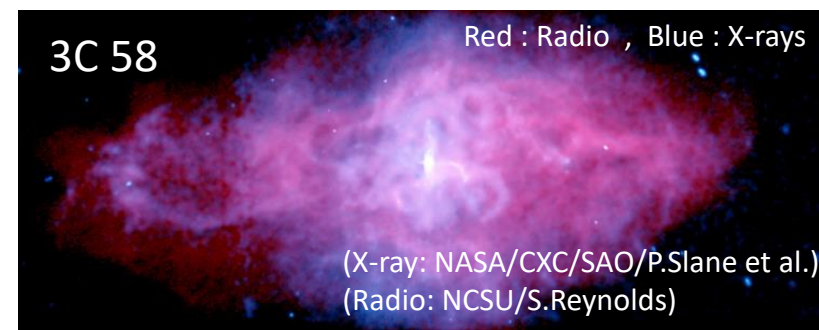
- Photon spectrum of entire nebula
  - Two breaks appear : intrinsic break & cooling break
  - Synchrotron spectrum is harder than IC
    - Due to the increasing magnetic field strength with radius  $r$  (In contrast,  $U_{ph}$  is uniform)



Application

# Target

- Selection criterion
  - Enough flux measurement at various frequencies
  - X rays PWN extend same as radio
- G21.5-0.9
  - Angular size : 40'' in radius
  - Distance :  $D=4.8\text{kpc}$  (Tian & Leahy 2008)
    - Nebula radius :  $r_N = 0.9\text{pc}$
  - Central pulsar : PSR J1833-1034
  - $P=61.9\text{ms}$  ,  $\dot{P} = 2.02 \times 10^{-13} \text{ss}^{-1}$ 
    - $L_{sd} = 3.3 \times 10^{37} [\text{erg/s}]$
- 3C 58
  - Angular size :  $5' \times 9'$
  - Distance :  $D=2.0\text{kpc}$  (Kothes et al.,2013)
    - Nebula radius :  $r_N = 2.0\text{pc}$
  - Central pulsar : PSR J0205+6449
  - $P=65.7\text{ms}$  ,  $\dot{P} = 1.94 \times 10^{-13} \text{ss}^{-1}$ 
    - $L_{sd} = 2.7 \times 10^{37} [\text{erg/s}]$





# Result -Entire Spectrum-

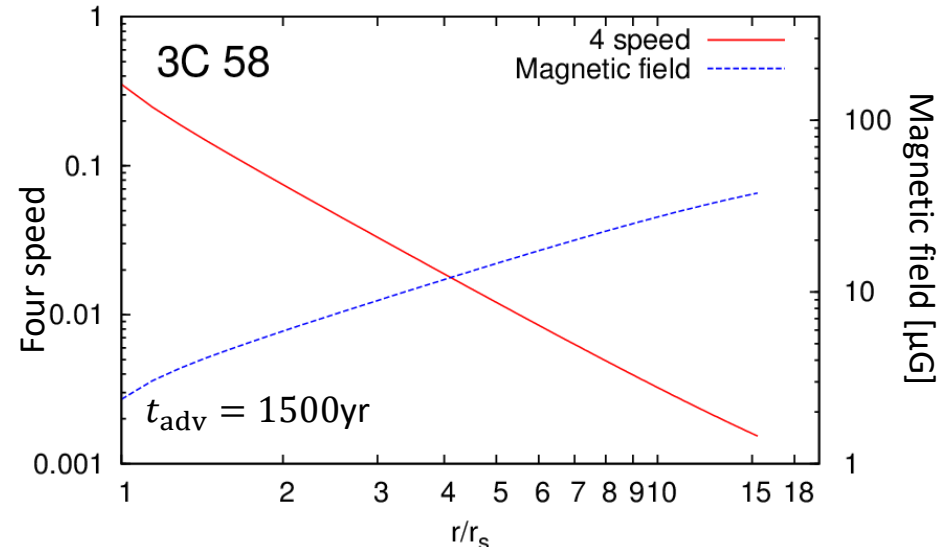
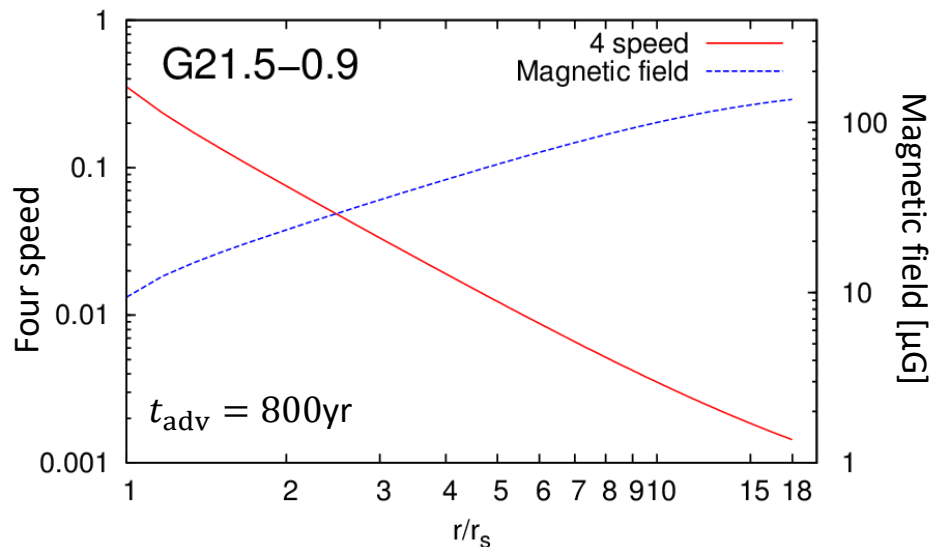
- Fitting

- Due to the enrichment of observational data, the model parameters can be obtained by fitting the entire spectrum only

- Note

- In GeV range, there is large systematic error caused by subtracting the contribution of the central pulsar
  - We regarded the Fermi detection of 3C 58 as upper limit
- There are NO natural parameter sets that can reproduce the X-ray index
  - We referred to only the absolute value of flux at X-ray datas

	G21.5-0.9	3C 58
$\sigma$	$2.0 \times 10^{-4}$	$1.0 \times 10^{-4}$
$r_s$	0.05 pc	0.13 pc
$E_b$	$5.0 \times 10^4 mc^2$	$6.0 \times 10^4 mc^2$
$p_2$	2.3	3.0



# Result -Entire Spectrum-

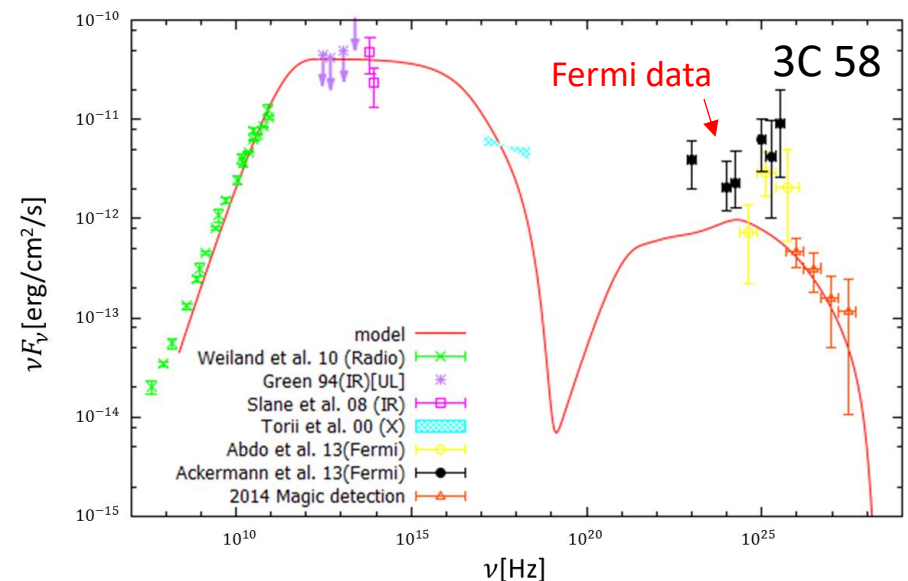
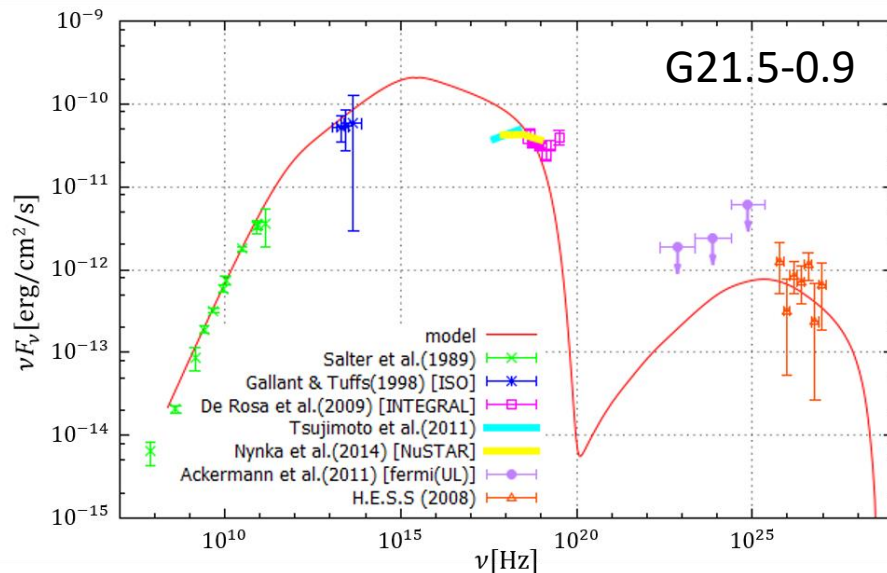
## • Fitting

- Due to the enrichment of observational data, the model parameters can be obtained by fitting the entire spectrum only

## • Note

- In GeV range, there is large systematic error caused by subtracting the contribution of the central pulsar
  - We regarded the Fermi detection of 3C 58 as upper limit
- There are NO natural parameter sets that can reproduce the X-ray index
  - We referred to only the absolute value of flux at X-ray datas

	G21.5-0.9	3C 58
$\sigma$	$2.0 \times 10^{-4}$	$1.0 \times 10^{-4}$
$r_s$	0.05 pc	0.13 pc
$E_b$	$5.0 \times 10^4 mc^2$	$6.0 \times 10^4 mc^2$
$p_2$	2.3	3.0

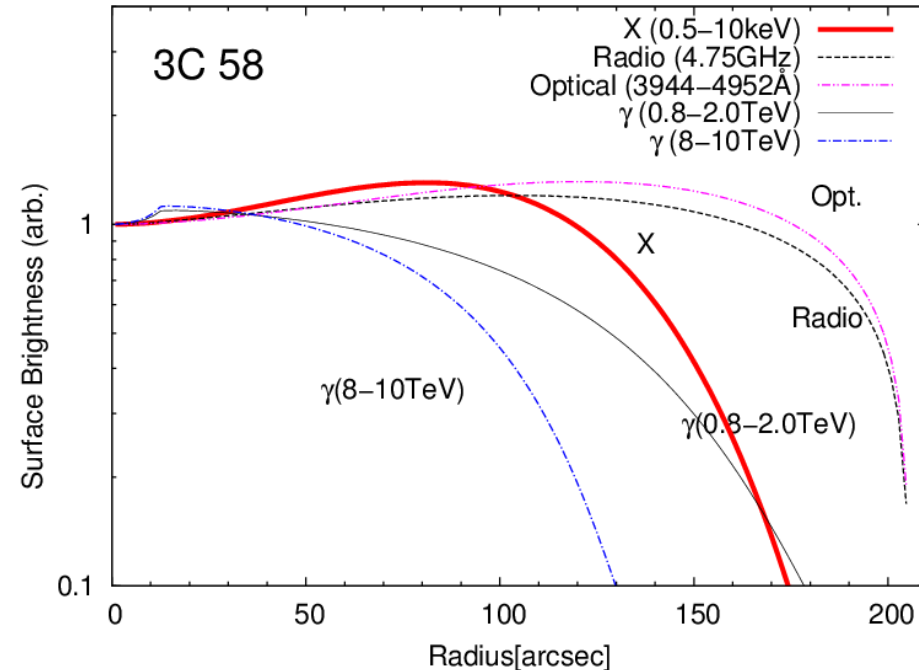
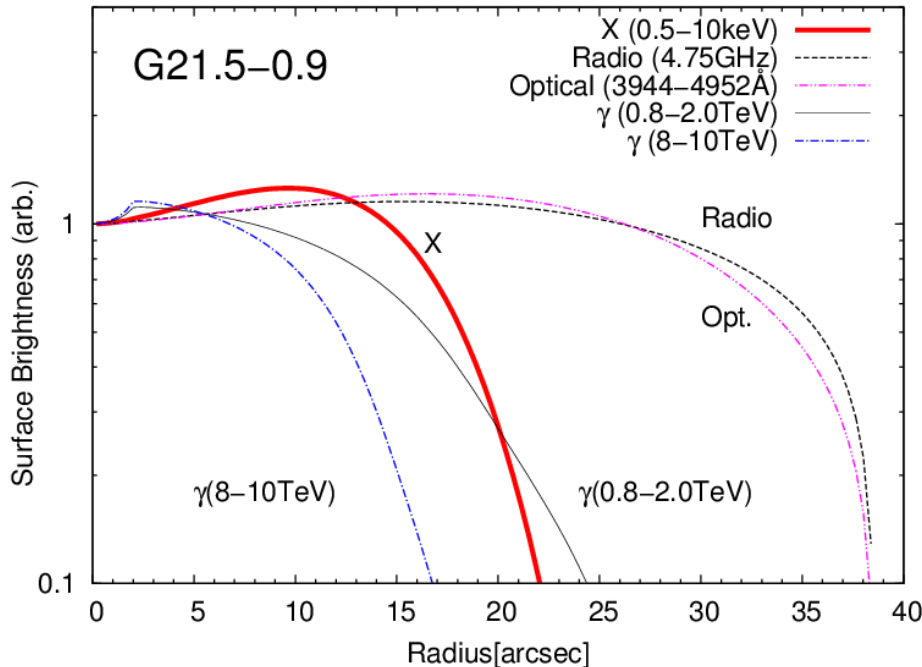


# Result -Surface Brightness-

- Surface brightness

- Radial profile of the surface brightness for various frequencies
- The Cut-off feature appears due to the two different reasons
  - At the edge of nebula -> “Confinement”
  - Inner nebula -> “Synchrotron Cooling”
- The X-rays nebulae are smaller than radio on both G21.5-0.9 and 3C 58

	G21.5-0.9	3C 58
$\sigma$	$2.0 \times 10^{-4}$	$1.0 \times 10^{-4}$
$r_s$	0.05 pc	0.13 pc
$E_b$	$5.0 \times 10^4 mc^2$	$6.0 \times 10^4 mc^2$
$p_2$	2.3	3.0

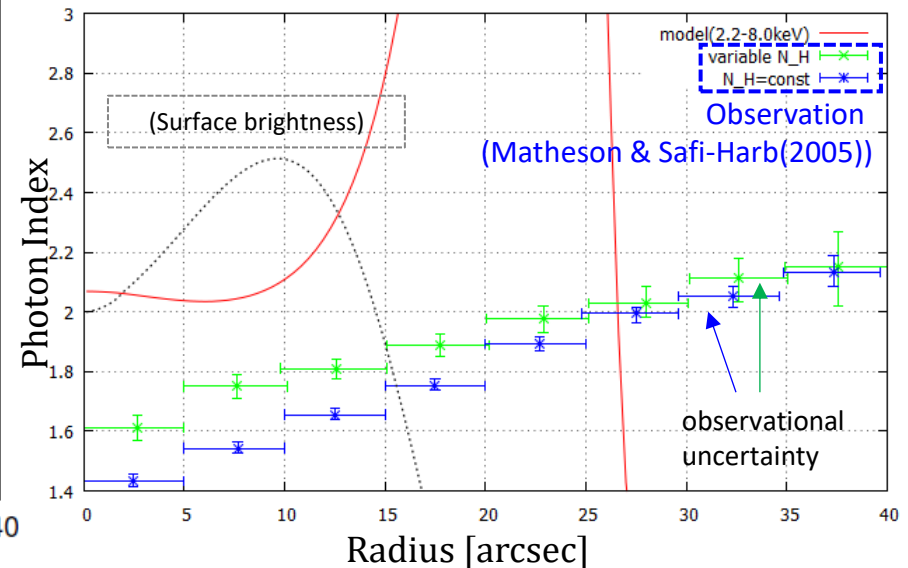
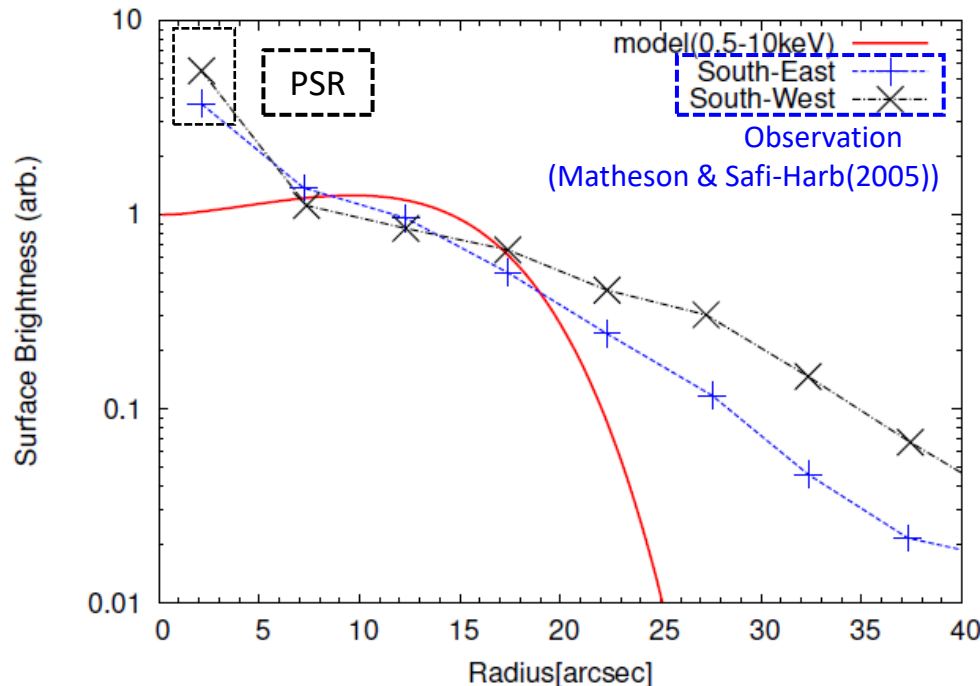
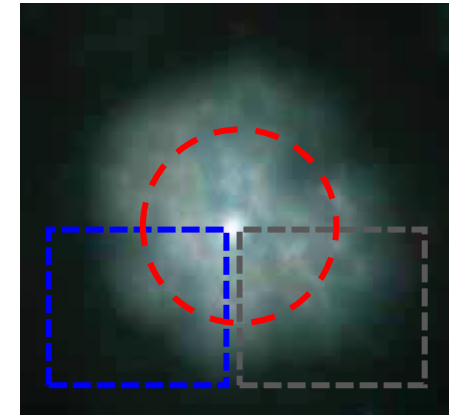


# Result -Surface Brightness-

- Comparison with observation
  - Surface brightness
    - Calculated emission region is smaller than observation
  - Photon index
    - The sudden steepening appears

The model can reproduce the entire nebula spectrum, BUT the spatial structure of emission is **incompatible**

	G21.5-0.9	3C 58
$\sigma$	$2.0 \times 10^{-4}$	$1.0 \times 10^{-4}$
$r_s$	0.05 pc	0.13 pc
$E_b$	$5.0 \times 10^4 mc^2$	$6.0 \times 10^4 mc^2$
$p_2$	2.3	3.0

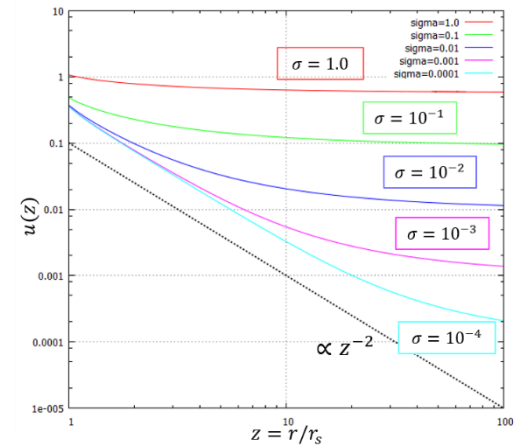


# Discussion & Conclusion



# Discussion –Parameter dependence-

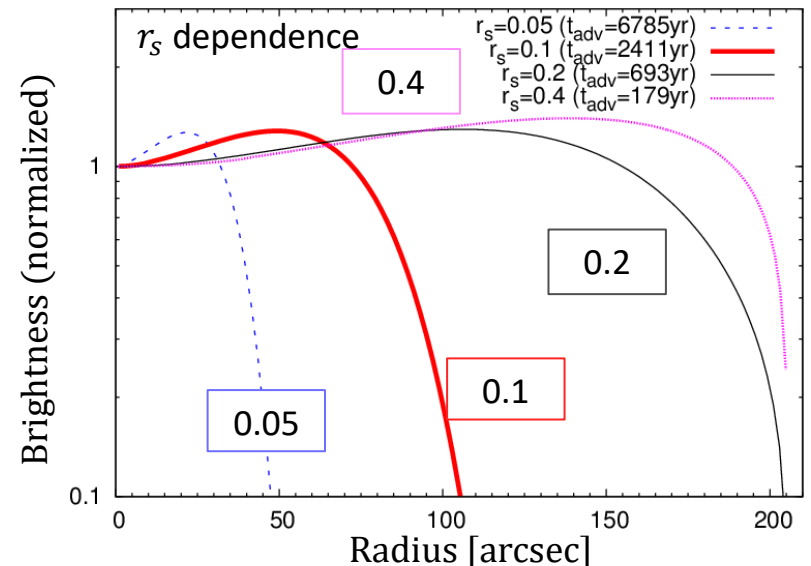
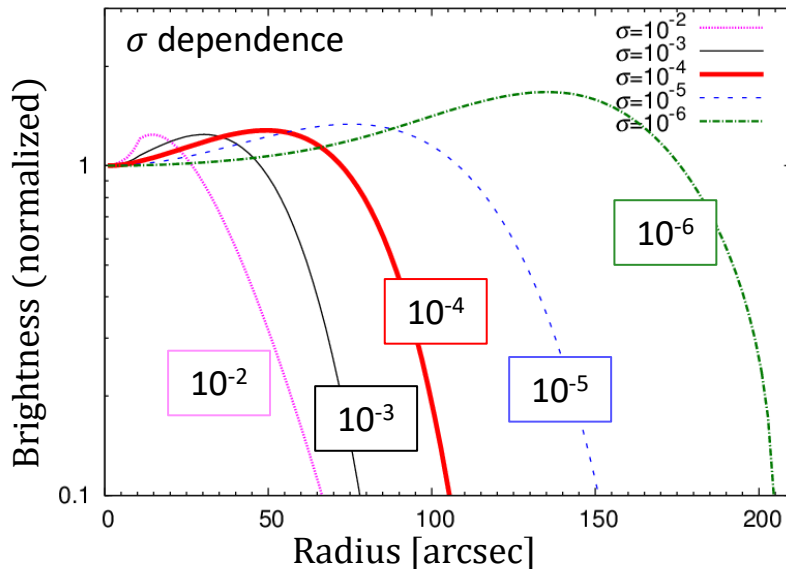
- Which parameter does change the emission profile?
  - $\sigma$  : determines the flow structure
  - $r_s$  : determines the characteristic scale of flow
  - Both  $\sigma$  and  $r_s$  are determines the strength of magnetic field
- The parameter dependence of surface brightness
  - $\sigma \rightarrow \text{small}$  : Magnetic field  $\searrow \Rightarrow$  Cooling becomes inefficient
  - $r_s \rightarrow \text{large}$  : Scale of spatial variation  $\nearrow$



$$B_1 = \sqrt{\frac{L_{sd}}{cr_s^2} \frac{\sigma}{1 + \sigma}}$$

$$\left(\frac{dE}{dt}\right)_{syn} = \frac{4}{3} \sigma_T c \gamma^2 U_B$$

To reproduce the larger X-ray PWN, smaller  $\sigma$  and larger  $r_s$  is required



# Discussion -Parameter dependence-

- Smaller  $\sigma$  and Larger  $r_s$ 
  - These mean to take the lower magnetic field
  - In the case of G21.5-0.9,

$$\frac{P_{\text{syn}}}{P_{\text{IC}}} \gtrsim 10 \Rightarrow B \gtrsim 30[\mu\text{G}] \text{ (c.f. Best-Fit } B \sim 120[\mu\text{G}])$$

The magnetic field expected by fitting entire spectrum is too strong to reproduce the observed expanse of the X-ray PWN.

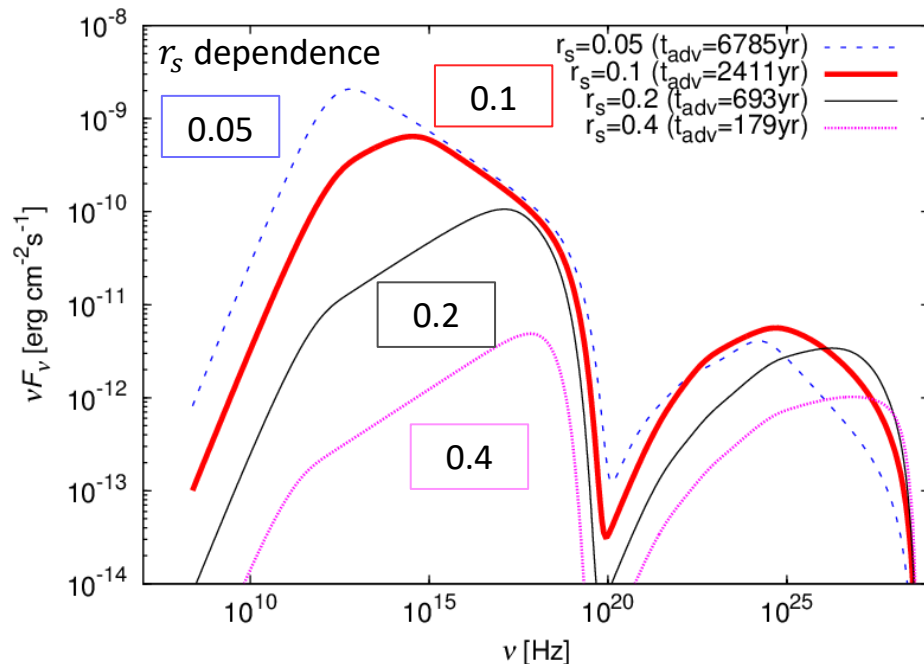
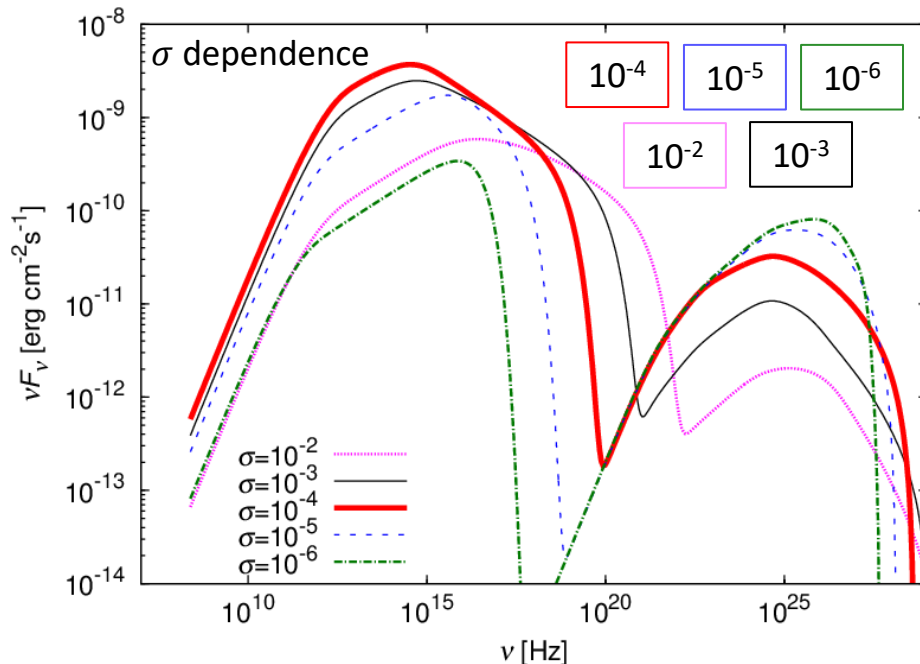
$\Rightarrow$  KC model CANNOT explain the spatial structure of PWNe!

$$B_1 = \sqrt{\frac{L_{sd}}{cr_s^2} \frac{\sigma}{1 + \sigma}}$$

$$\left(\frac{dE}{dt}\right)_{\text{syn}} = \frac{4}{3} \sigma_T c \gamma^2 U_B$$

$$\left(\frac{dE}{dt}\right)_{\text{IC}} = \frac{4}{3} \sigma_T c \gamma^2 U_{\text{ph}}$$

$$\frac{P_{\text{syn}}}{P_{\text{IC}}} = \frac{U_B}{U_{\text{ph}}} \propto \sigma r_s^{-2}$$

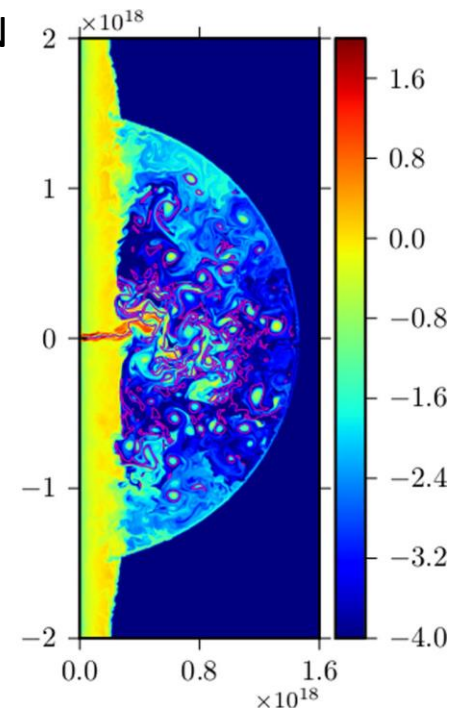


# Summary

- We investigate the 1-D model of PWNe based on Kennel & Coroniti (1984), and apply this model to two objects, G21.5-0.9 and 3C58.
- We find that the KC model can reproduce the entire spectrum but the spatial structure (surface brightness and photon index) is incompatible.
- In this model, the magnetic field required by the entire spectrum is too strong to reproduce the spatial structure of emission.
- That is to say, the high-energy electrons that emits the X-rays suffer the excessive synchrotron cooling.

# Future Work

- Observational study
  - The low energy component of electrons does not suffer synchrotron cooling.
    - ⇒ Observing PWNe by radio, we can obtain the information about the spatial structure of the magnetic field and electron density. BUT these degenerates.
  - If we investigate the spatial structure by  $\gamma$ -rays, we can obtain the spatial distribution of electrons independently
    - ⇒ CTA will achieve the spatially resolved observation of PWN
- Improvement of the model
  - Recent study by MHD simulation implies the existence of turbulence in PWN (e.g. Porth+14)
  - Approach
    - Diffusion: Spatial diffusion by disturbed magnetic field
      - ⇒ This will spread the high-energy electrons further
    - Re-acceleration : Stochastic acceleration by turbulence
      - ⇒ This will suppress the synchrotron cooling



(Porth et al. ,2014)

